Article

Cancer Cell

Fasting-Mimicking Diet Reduces HO-1 to Promote T Cell-Mediated Tumor Cytotoxicity

Graphical Abstract

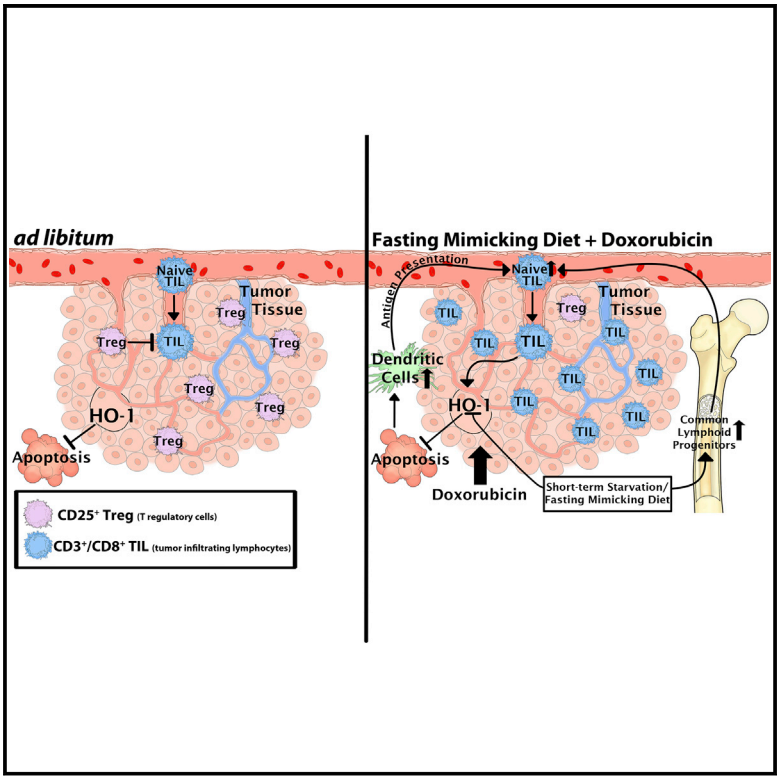

Authors

Stefano Di Biase, Changhan Lee, Sebastian Brandhorst, ..., Min Wei, Todd E. Morgan, Valter D. Longo

Correspondence

vlongo@usc.edu

In Brief

Di Biase et al. show that combining a fasting-mimicking diet with chemotherapy increases the levels of bone marrow common lymphoid progenitor cells and cytotoxic $CD8^+$ tumor-infiltrating lymphocytes, delaying tumor progression. In breast tumors, this effect is partially mediated by downregulating HO-1.

Highlights

- The FMD is as effective as fasting in sensitizing tumors to chemotherapy
- FMD cycles promote the enrichment of common lymphoid progenitor cells
- FMD/doxorubicin increase tumor immunogenicity and tumor-infiltrating lymphocytes
- HO-1 plays a key role in the FMD-induced chemosensitization of breast cancer cells

Accession Numbers

GSE28556

Di Biase et al., 2016, Cancer Cell *30*, 136–146
July 11, 2016
http://dx.doi.org/10.1016/j.ccell.2016.06.005

CellPress

Cancer Cell
Article

Fasting-Mimicking Diet Reduces HO-1 to Promote T Cell-Mediated Tumor Cytotoxicity

Stefano Di Biase,[1,4] Changhan Lee,[1,4] Sebastian Brandhorst,[1] Brianna Manes,[1] Roberta Buono,[1] Chia-Wei Cheng,[1] Mafalda Cacciottolo,[1] Alejandro Martin-Montalvo,[2] Rafael de Cabo,[2] Min Wei,[1] Todd E. Morgan,[1] and Valter D. Longo[1,3,*]

[1]Longevity Institute, Leonard Davis School of Gerontology and Department of Biological Sciences, University of Southern California, Los Angeles, CA 90089, USA

[2]Translational Gerontology Branch, National Institute on Aging, National Institutes of Health, Baltimore, MD 21224, USA

[3]IFOM, FIRC Institute of Molecular Oncology, Milan 20139, Italy

[4]Co-first author

*Correspondence: vlongo@usc.edu

http://dx.doi.org/10.1016/j.ccell.2016.06.005

SUMMARY

Immune-based interventions are promising strategies to achieve long-term cancer-free survival. Fasting was previously shown to differentially sensitize tumors to chemotherapy while protecting normal cells, including hematopoietic stem and immune cells, from its toxic side effects. Here, we show that the combination of chemotherapy and a fasting-mimicking diet (FMD) increases the levels of bone marrow common lymphoid progenitor cells and cytotoxic $CD8^+$ tumor-infiltrating lymphocytes (TILs), leading to a major delay in breast cancer and melanoma progression. In breast tumors, this effect is partially mediated by the downregulation of the stress-responsive enzyme heme oxygenase-1 (HO-1). These data indicate that FMD cycles combined with chemotherapy can enhance T cell-dependent targeted killing of cancer cells both by stimulating the hematopoietic system and by enhancing $CD8^+$-dependent tumor cytotoxicity.

INTRODUCTION

Immune cells act as sentinels that recognize peptides originating from mutated genes and eliminate malignant and possibly pre-malignant cells (Rock and Shen, 2005). Cancer immunotherapy exploits this property of the immune system to recognize and eliminate cancer cells (Vesely et al., 2011; Zitvogel et al., 2008) by triggering the activation of inherent antitumor T cells (Pardoll, 2012; Wolchok et al., 2013) or through the reintroduction of engineered T cells into patients (Burns et al., 2010; Maude et al., 2014). The importance of a healthy immune system is underlined by the fact that immunosuppressed/immunocompromised subjects are at a higher risk for cancer (Zitvogel et al., 2006). Moreover, some traditional cytotoxic chemotherapeutics rely on the cooperation of the patient's immune system to eliminate cancer cells (Alizadeh et al., 2014; Arinaga et al., 1986; Bracci et al., 2014).

The immunosuppressive effect of some standard interventions, including radiotherapy and chemotherapy (Weinblatt et al., 1985; Weiner and Cohen, 2002), can compromise their therapeutic efficacy (Balow et al., 1975; Rasmussen and Arvin, 1982). Such therapeutic inefficacy and tumor resistance can also be caused by regulatory T cells (Tregs), which can suppress the lymphocytic activity through a mechanism mediated by heme oxygenase-1 (HO-1) (Choi et al., 2005; El Andaloussi and Lesniak, 2007). Conversely, some chemotherapeutics, such as anthracyclines, are known to stimulate the recognition of cancer cells by the immune system (Arinaga et al., 1986; Casares et al., 2005; Orsini et al., 1977), which may potentiate the effect of some immune-based therapies.

Significance

Cancer immunotherapy is a promising intervention for the targeted killing of tumor cells. However, tumor-localized immunosuppression induced by cancer cells (immunoresistance) often leads to limited T cell-mediated cytotoxicity. Moreover, chemotherapy- and radiotherapy-induced immunosuppression can further reduce the efficacy of immune-based treatments. Here we show that a fasting-mimicking diet (FMD) increases the levels of common lymphoid progenitor cells (CLPs) and of circulating $CD8^+$ lymphocytes. The combination of the FMD and doxorubicin increased the number of cytotoxic $CD8^+$ tumor-infiltrating lymphocytes (TILs). The FMD-induced recruitment of TILs was mediated by heme oxygenase-1 (HO-1) and was significantly correlated with a lower number of regulatory T cells in the tumor bed. Thus, the FMD is a promising intervention to potentiate immune-based and standard cancer therapies.

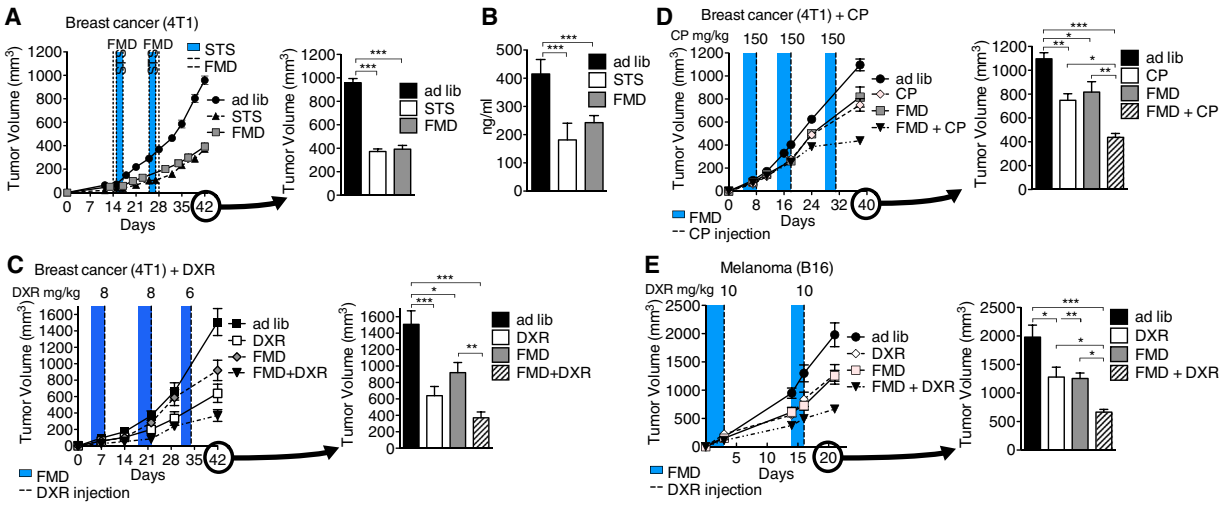

Figure 1. A Fasting-Mimicking Diet Alone or in Combination with Chemotherapy Is as Effective as Short-Term Starvation in Reducing Tumor Progression

(A–D) 12-week-old female BALB/c mice were grafted with breast cancer (4T1) cells and subjected to (A) multiple cycles of FMD or STS alone, or to a combination of FMD and the chemotherapy drugs (C) doxorubicin (DXR) or (D) cyclophosphamide (CP). (B) Circulating IGF-1 levels at the end of STS or FMD in (A) were measured.

(E) 12-week-old female C57BL/6 mice were grafted with melanoma (B16) cells and subjected to multiple cycles of FMD alone or in combination with DXR. Tumor volume at multiple time points (on the left) and immediately before euthanasia (on the right) are reported for each set of treatments. The animals receiving chemotherapy were injected at the end of each FMD cycle (shaded area).

(A and B) n = 10, (C) n = 13, (D) n = 10, and (E) n = 15. Data are represented as means ± SEM. One-way ANOVA (Tukey's post-analysis test) was performed. *p < 0.05, **p < 0.01, and ***p < 0.001. See also Figure S1.

We have previously shown that short-term starvation (STS) can selectively sensitize cancer cells to chemotherapeutics (differential stress sensitization [DSS]), while simultaneously protecting normal cells from their side effects (differential stress-resistance [DSR]) (Lee et al., 2012; Raffaghello et al., 2008) via the insulin-like growth factor 1 (IGF-1) pathway and the regulation of glucose levels (Lee et al., 2010). Recently, we also reported that STS promotes hematopoietic stem cell (HSC) self-renewal and reverses chemotherapy-induced immunosuppression (Cheng et al., 2014). Because water-only STS is challenging for mice and cancer patients, we have developed a fasting-mimicking diet (FMD) that is low in calories, protein, and sugar (Brandhorst et al., 2015). This FMD reduces circulating IGF-1 and glucose, two major factors involved in DSR and DSS, to levels similar to those observed during STS (Brandhorst et al., 2015). Here, we tested the effect of this FMD in combination with chemotherapy on the immune system, and on the immunogenicity of cancer cells.

RESULTS

A FMD Alone or in Combination with Chemotherapy Is as Effective as STS in Reducing Tumor Progression

We have previously shown that STS is safe and effective in inducing DSS via IGF-1 signaling (Lee et al., 2012; Raffaghello et al., 2008; Safdie et al., 2009). Here we tested the efficacy of cycles of the FMD (Brandhorst et al., 2015) in inducing DSS in a syngeneic murine breast cancer (4T1) model (Figure S1). Four days of FMD feeding were as effective as 2 days of STS in retarding tumor growth and reducing circulating IGF-1 in the absence of chemotherapy (Figures 1A and 1B), and in sensitizing cancer cells to doxorubicin (DXR) and cyclophosphamide (CP) (Figures 1C, 1D, S2C, and S2D) (Lee et al., 2010, 2012; Raffaghello et al., 2008). Similar effects of the FMD were also observed in a murine melanoma (B16) model, in which mice were treated with DXR (Figure 1E). The combination of the FMD and DXR/CP had an additive effect on tumor suppression, causing a 3-fold reduction in tumor volume compared with that observed in mice fed ad libitum (Figures 1C–1E).

FMD in Combination with DXR Promotes Accumulation of Tumor-Infiltrating Lymphocytes in the Tumor Bed

STS promotes HSC self-renewal and reverses chemotherapy-induced immunosuppression (Cheng et al., 2014). As previously reported (Cheng et al., 2014), three cycles of the FMD also caused a 33% increase in $CD8^+$ circulating lymphocytes (Figure S2A) and a 2-fold increase in common lymphoid progenitor cells (CLP) in the bone marrow (Figures 2A and S2B). This increase, likely due to HSC regeneration following re-feeding after STS (Cheng et al., 2014), raises the possibility that the immune system may be involved in mediating FMD-dependent DSS.

To evaluate whether FMD cycles could promote tumor immunogenicity, we measured the level of tumor-infiltrating lymphocytes (TILs) after three cycles of FMD + DXR in mice. Only the combination of FMD + DXR significantly increased the number of $CD3^+/CD8^+$ TILs, as determined by both immunohistochemistry (Figures 2B and S2E–S2J) and fluorescence-activated cell-sorting analysis (Figures 2C–2E), but there were no significant changes in the number of $CD3^-/CD8^+$ cells (Figure S2K). $CD3^+$ cell infiltration increased after the first FMD cycle (Figures S2E–S2G), whereas $CD8^+$ cell infiltration increased after the third

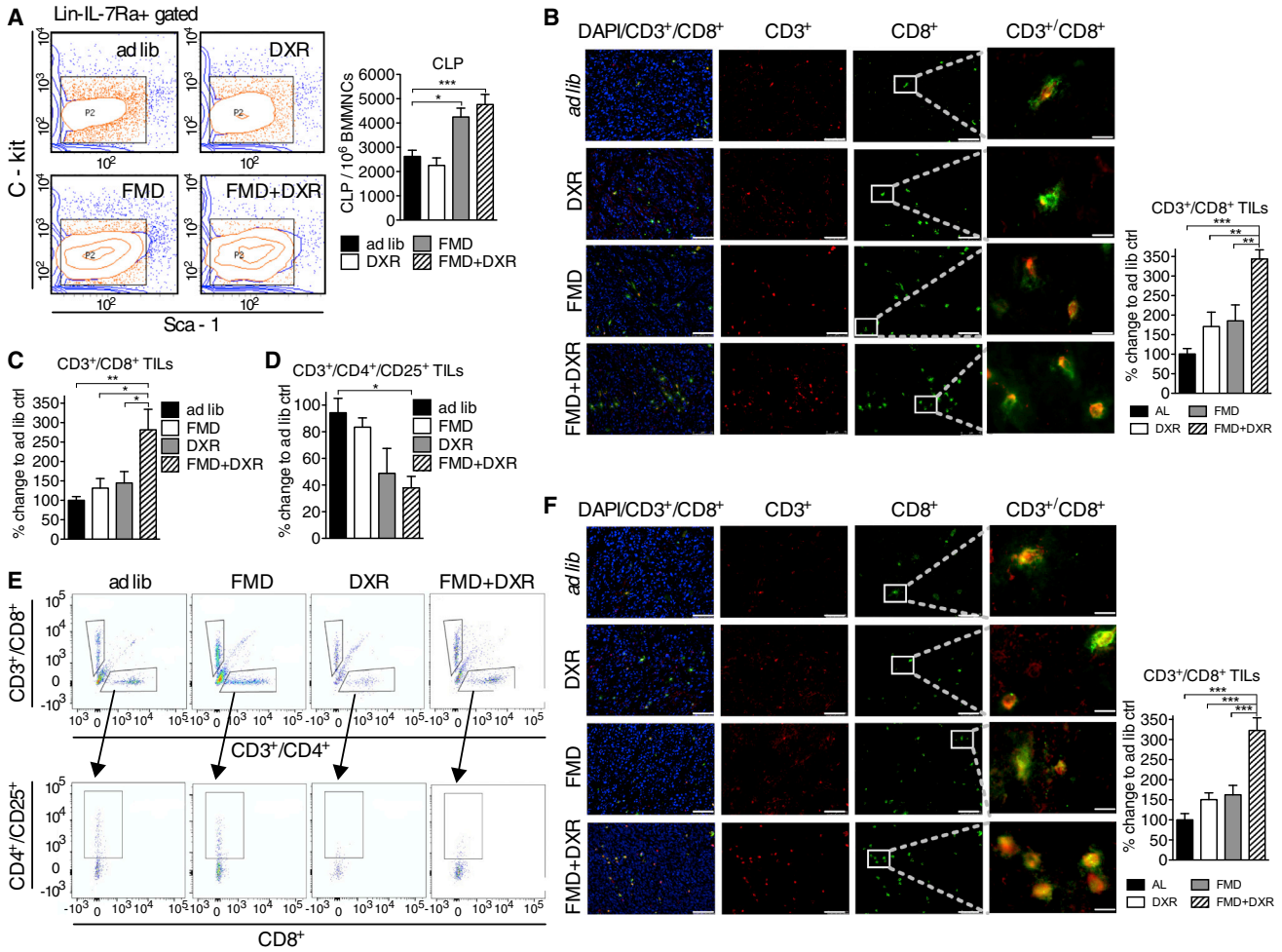

Figure 2. FMD in Combination with Doxorubicin Promotes Accumulation of Tumor-Infiltrating Lymphocytes in the Tumor Bed

(A) Bone marrow collected from BALB/c mice undergoing FMD/DXR treatments (see Figure S3A) was collected at the end of the experiment and analyzed with fluorescence-activated cell sorting (FACS) (n = 6) to assess the levels of common lymphoid progenitors (CLP).

(B) Breast cancer (4T1) tumor tissues collected at the end of the experiment (see Figure S3A) were analyzed using immunohistochemistry to assess $CD3^+/CD8^+$ TILs (n = 8) (quantification on the right).

(C, E) $CD3^+/CD8^+$ and (D, E) $CD3^+/CD4^+/CD25^+$ were also assessed by FACS analysis (n = 7) in tumor tissue collected from a separate, equivalent experiment (see Figure 1C).

(F) Melanoma (B16) tissue collected (see Figure 1E) was also processed to assess the levels of TILs (quantification on the right). Scale bar for DAPI, CD3, and CD8 is 75 μm. Scale bar for $CD3^+/CD8^+$ is 12.5 μm.

Data are represented as means ± SEM. The significance of the differences between experimental groups was determined by using one-way ANOVA (Tukey's post-analysis test). *p < 0.05, **p < 0.01, and ***p < 0.001. See also Figure S2.

FMD cycle, only in combination with DXR (Figures S2H–S2J). The cytotoxic activity of TILs was reflected by increased levels of granzyme B and apoptosis in tumor cells, and by reduced tumor size (Figure S3). Similarly, higher levels of $CD3^+/CD8^+$ TILs were observed in C57BL/6 mice bearing melanoma (B16) that underwent FMD + DXR treatment (Figures 1E and 2F).

$CD3^+/CD8^+$ Lymphocytes are Key in FMD-Mediated DSS to Chemotherapy

$CD3^+/CD8^+$ TILs are tumor-killing effector immune cells, which serve as an indicator of favorable prognosis (Andre et al., 2013; Issa-Nummer et al., 2013). To test whether $CD3^+/CD8^+$ TILs are required for FMD-induced tumor sensitization, we examined immunocompromised *nude* BALB/c mice that are athymic and therefore do not produce T lymphocytes. In contrast to the results in immunocompetent mice, the FMD was not effective in reducing tumor progression in *nude* mice (Figure 3A), and showed no changes in granzyme B or cleaved caspase-3 levels (Figures S4A–S4E). Nonetheless, the FMD successfully protected *nude* mice against DXR-dependent and tumor-independent toxicity (Figure 3B) (Raffaghello et al., 2008), indicating that the FMD-induced protection of normal cells, unlike tumor sensitization, is not affected by T lymphocyte function.

To directly test the role of TILs in mediating the FMD-dependent sensitization of tumors to DXR, we selectively depleted $CD8^+$ T lymphocytes using a neutralizing monoclonal antibody

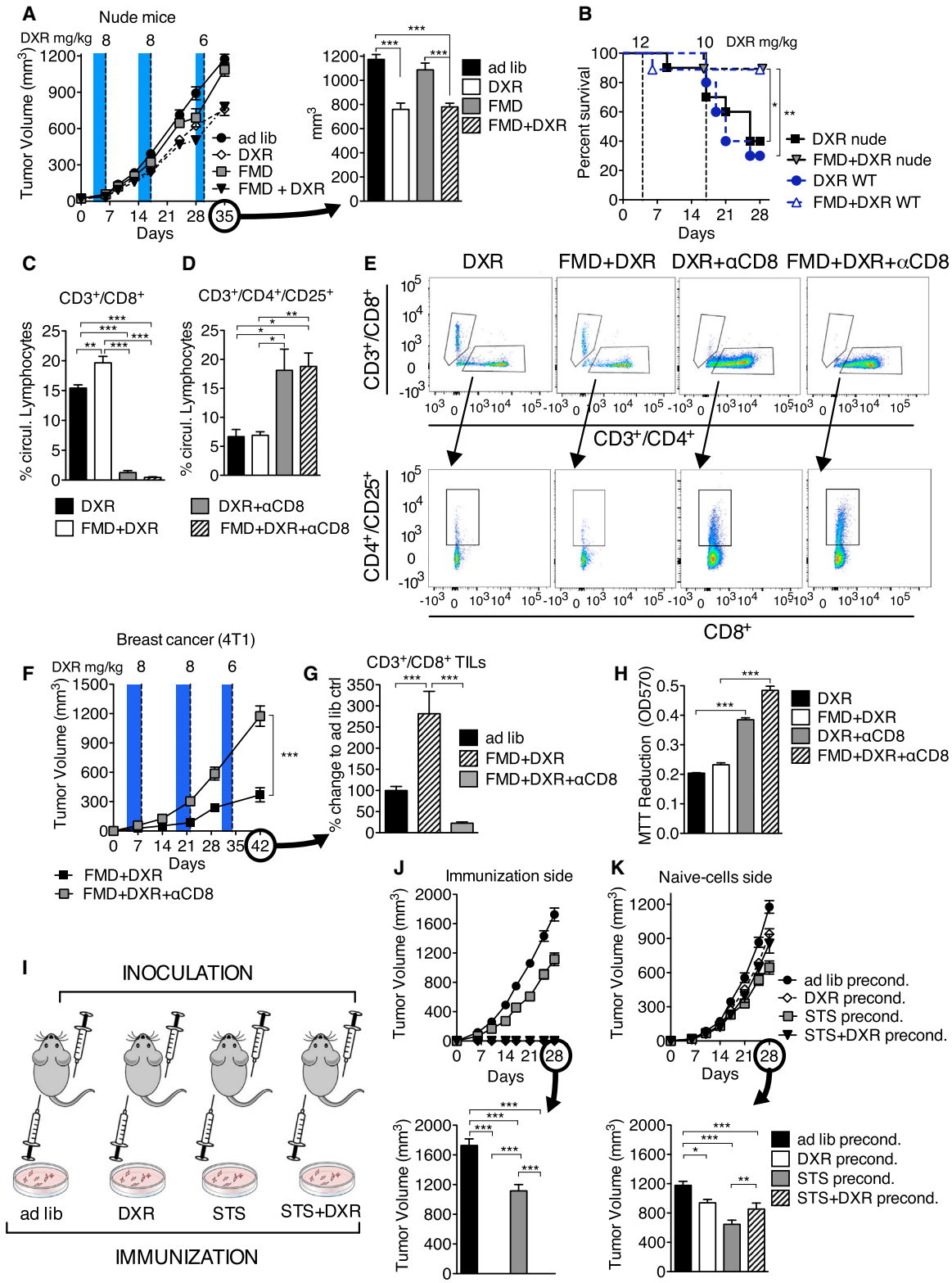

Figure 3. CD3⁺/CD8⁺ Lymphocytes Have a Key Role in FMD-Mediated Differential Stress Sensitization to Chemotherapy

(A) The effect of FMD on breast tumor growth (4T1) in immunodeficient BALB/c *nude* mice (n = 15) (see Figure S4A–S4E).

(B) The survival of wild-type (WT) and *nude* mice injected with high doses of DXR and undergoing the ad libitum or FMD regimens.

(C–H) 4T1 breast tumor-bearing mice were treated with DXR, FMD + DXR alone or in combination with αCD8 monoclonal antibody and (C–E) circulating levels of (C, E) $CD3^+/CD8^+$ and (D, E) $CD3^+/CD4^+/CD25^+$ were determined by FACS (n = 7).

(legend continued on next page)

(αCD8; clone YTS 169.4) (Carmi et al., 2015) or IgG (control) (Figures 3C and 3E). Notably, the depletion of $CD8^+$ circulating cells was also associated with an increase in the number of Tregs (Figures 3D and 3E). The antibody-dependent depletion of $CD8^+$ T lymphocytes reversed the effects of FMD + DXR on the progression of grafted breast tumors (Figures 3F and 3G). Furthermore, lymphocytes isolated from αCD8 antibody-treated mice caused significantly less cytotoxicity to 4T1 cells in vitro compared with those from IgG-treated mice (Figure 3H).

These results indicate that activated TILs are important for the FMD-dependent sensitization of breast cancer cells to chemotherapeutics.

Anthracyclines can increase cancer cell immunogenicity and attract cytotoxic T lymphocytes (CTLs) to the tumor (Michaud et al., 2011). To test whether the FMD directly increases tumor immunogenicity, we cultured breast cancer cells (4T1) in FMD-like conditions (referred to as STS for in vitro experiments and consisting of reduced glucose/serum) and DXR before grafting them into immunocompetent mice. One week after grafting the pre-conditioned breast cancer cells, all mice were also grafted with naive breast cancer cells on the other flank (Figure 3I). Although all mice were ''immunized'' by grafting the same number of live pre-conditioned breast cancer cells, the DXR and STS + DXR groups did not develop tumors (Figures 3J and S4F). Consistent with previous studies (Casares et al., 2005; Inoue et al., 2014), naive tumors on the other flank displayed retarded growth after 4 weeks in mice grafted with cells pre-cultured with DXR (Figure 3K). Notably, STS pre-conditioning alone was more effective than STS + DXR, possibly because the less severe apoptotic effects of the STS allowed the immunogenic cancer cells to live longer and therefore provide a prolonged immunogenic stimuli after grafting in mice (Figures 3J, 3K, and S4F).

Collectively, these results indicate that FMD (i.e., STS in vitro) increased DXR-dependent tumor immunogenicity and expanded the pool of $CD8^+$ TILs needed to effectively target tumors.

HO-1 Is a Mediator of FMD/STS-Dependent DSS

We performed microarray analysis to identify STS-dependent effects on the differential expression in normal and cancer cells of genes that may be relevant to TIL-dependent toxicity, and identified the inducible stress-responsive protein HO-1 as a potential candidate (Figure S5A). Thereafter, we confirmed that both STS and FMD reduced the expression of HO-1 in the grafted breast tumors (Figure 4A). On the contrary, STS differentially increased HO-1 expression in normal tissues (Figure 4A). Notably, the expression of Nrf2, an upstream regulator of HO-1, was also differentially reduced in the grafted breast tumors following STS (Figure S5B). Similar effects on HO-1 expression were also observed in vitro (Figures 4B, S5C, and S5D), specifically in the nucleus (Figure S5E). In fact, cancer cells have been reported to show increased levels of nuclear HO-1 independent of its enzymatic activity (Hsu et al., 2015).

To test the role of HO-1 in FMD-mediated DSS, we cultured 4T1 cancer cells in normal or FMD-like conditions (referred to as STS for in vitro experiments and consisting of reduced glucose/serum) and exposed them to the HO-1 activator hemin or its inhibitor zinc protoporphyrin (ZnPP) in the presence of CP or DXR. The induction of HO-1 using hemin (Figures 4C, 4E, and S5F) or its overexpression by stably transfecting a pHO-1 construct (Suliman et al., 2007) (Figures S5G and S5H) in breast cancer cells (4T1) partially reversed the STS-induced sensitization to DXR and CP in vitro (Figures 4D and 4F). Conversely, the HO-1 inhibitor ZnPP sensitized breast cancer cells (4T1) to CP under normal conditions in vitro (Figure 4G). Thus, the downregulation of HO-1 is important for FMD-dependent DSS.

Downregulation of HO-1 in the Tumor by FMD/STS Is Necessary To Decrease Tregs and for the Immune-Dependent Targeting of Cancer Cells

HO-1 is known to confer protection against oxidative damage and apoptosis (Chen et al., 2004), promote tumor progression (Hirai et al., 2007; Liu et al., 2011; Metz et al., 2010), and have immunomodulatory roles that affect various T cell subpopulations including Tregs (Brusko et al., 2005; Xia et al., 2008). In mice, HO-1 inhibitor ZnPP (40 mg/kg/day intraperitoneally [i. p.]) treatment was as effective as STS in retarding breast tumor progression (4T1) (Figure 5A). In agreement with the in vitro results, concurrent hemin treatment (30 mg/kg/day i.p.) reversed STS-induced retardation of breast tumors (4T1), whereas hemin alone did not show significant responses (Figure 5B). Both the induction and overexpression of HO-1 (by hemin or stable transfection, respectively), and the $CD8^+$ CTL depletion reversed the FMD-induced (1) sensitization of breast tumors (4T1) to DXR (Figures 5C, 5D, and 6A) and (2) accumulation of $CD3^+$/$CD8^+$ TILs (Figures 6B and 6D). Interestingly, HO-1 induction/overexpression also increased $CD3^+/CD4^+/CD25^+$ Tregs and, to a much smaller extent, $CD3^+/CD8^+/CD25^+$ Tregs in the tumor (Figures 6C, 6D, and S5K). Similar effects were observed after CP treatment (Figure S6). As expected, $CD8^+$ CTL depletion alone was not associated with increased levels of tumor-associated Tregs (Figure 6C). In mammalian cells, HO-1 is a rate-limiting enzyme catalyzing the degradation of heme to produce carbon monoxide (CO), free iron, and biliverdin (Maines, 1988).

(F) Tumor volumes of FMD + DXR and FMD + DXR + αCD8 were measured at multiple time points.

(G) TILs were also assessed in tumor samples collected from the same animals.

(H) Circulating lymphocytes from DXR, FMD + DXR, DXR + αCD8, and FMD + DXR + αCD8. These animals were collected and cultured ex vivo with 4T1 cells for 24 hr and viability was assessed by MTT reduction.

(I) Mice were immunized by subcutaneous inoculation (in the left flank) with 4T1 breast cancer cells pre-conditioned in vitro with either ad libitum (2 g/l glucose + 10% FBS) or STS medium (0.5 g/l glucose + 1% FBS) with or without DXR (5 μM). 7 days after the immunization, the same animals were inoculated with naive 4T1 cells in the right flank (n = 10).

(J and K) Tumor progression for the immunization (left) and the naive (right) sides are reported.

Data are represented as means ± SEM. One-way ANOVA (Tukey's post-analysis test) and log rank (Mantel-Cox) test (survival) was performed. Comparisons between groups were performed with Student's t test. *$p < 0.05$, **$p < 0.01$, and ***$p < 0.001$. See also Figure S3.

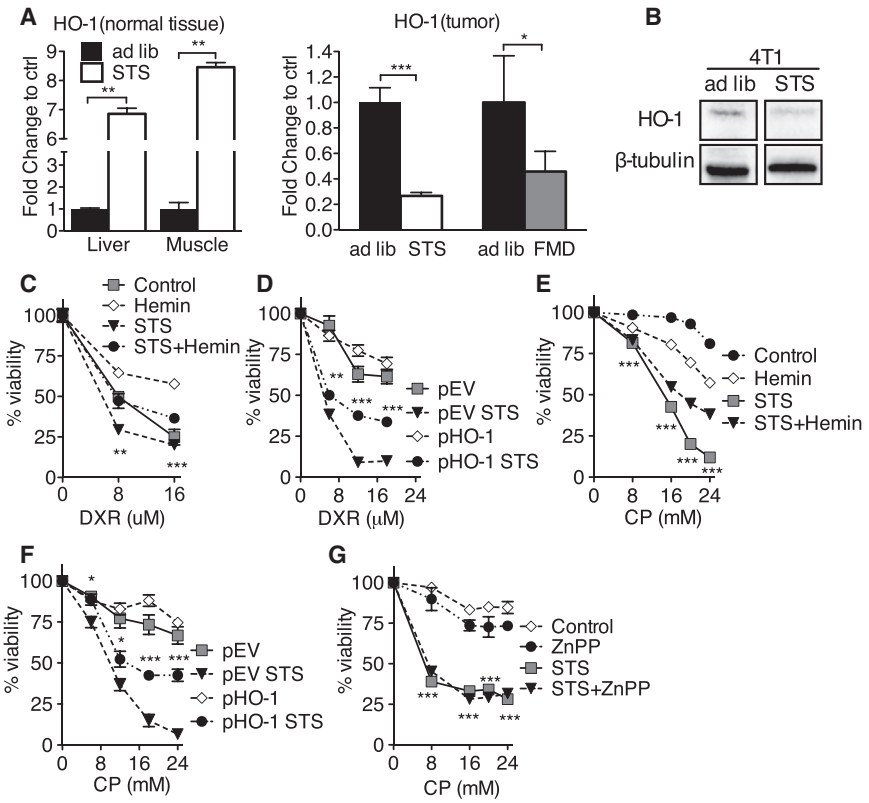

Figure 4. Heme Oxygenase-1 Has a Key Role in Mediating STS-dependent Differential Stress Sensitization

(A) HO-1 expression levels of grafted 4T1 tumor and normal (liver and skeletal muscle) tissues collected from mice fed ad libitum and mice undergoing the STS or FMD regimens were analyzed with qRT-PCR.

(B) HO-1 levels in 4T1 cells following 48 hr of in vitro STS were measured by western blotting (n = 3) (the blots were captured with Bio-Rad ChemiDoc), and unedited, representative bands are shown.

(C, E, and G) Viability of 4T1 cells was determined by MTT reduction following (C) DXR and hemin (10 μM), (E) CP and hemin (10 μM), and (G) CP and ZnPP (20 μM).

(D and F) Viability of 4T1 cell stably overexpressing HO-1 (pHO-1) or empty vector (pEV) was determined by MTT following (D) DXR and (F) CP under control and STS conditions.

Data are represented as means ± SEM. The significance of the differences between experimental groups was determined using one-way ANOVA (Tukey's post-analysis test). Comparisons between groups were performed using Student's t test. *p < 0.05, **p < 0.01, and *** p < 0.001. See also Figure S5.

Biliverdin can have antioxidative effects (Abraham and Kappas, 2008; Otterbein et al., 2000), but its treatment alone was not sufficient to reverse the FMD-dependent DSS (Figures S5I and S5J), suggesting a more complex involvement of the HO-1 pathway. Because HO-1-dependent increase of CO has been shown to interfere with angiogenesis (Ahmad et al., 2015), metastasis (Tertil et al., 2015), and tumor growth (Wegiel et al., 2013) it will be important to further study the potential role of CO in the antitumor effects of the FMD.

These results indicate that reduced HO-1 expression in tumors mediates, in part, the anticancer effect of FMD by increasing $CD8^+$ TIL-dependent cytotoxicity, which may be facilitated by downregulation of Tregs.

DISCUSSION

We provide evidence that the FMD-dependent DSS is, in part, mediated by $CD8^+$ TIL-dependent killing of cancer cells, associated with an increase in lymphoid progenitor cells.

Immunological approaches are among the most promising treatments, with the potential to result in cancer-free survival. However, immunotherapies are expensive and often effective only in a subset of patients. Here we show that fasting can be substituted with a low calorie and protein FMD, which provides high nourishment and is effective in inducing the targeted killing of cancer cells. The efficacy of the FMD can be enhanced when it is administered in combination with various chemotherapeutics. The efficacy of fasting in inducing DSS both in in vitro and in vivo models has been extensively reported in recent years and has been proposed to be mediated, in part, by the reduction of circulating IGF-1 and glucose levels (Lee et al., 2010, 2012; Raffaghello et al., 2008). Our study shows that T cells can play a key role in the killing of breast cancer cells during FMD/STS. Another important component of the antitumor activity triggered by FMD/STS appears to be its effect on the repopulation of the bone marrow with CLPs (Cheng et al., 2014). Our work extended from the systemic benefits of the FMD on the immune system to those promoting a targeted killing of cancer cells. Because of the strong association between the presence of $CD3^+/CD8^+$ TILs in the tumor bed and a positive outcome of the cancer treatment (Andre et al., 2013; Issa-Nummer et al., 2013), our results are of potential therapeutic relevance as they show the effect of a safe and inexpensive regimen in improving the efficacy of cancer therapy by stimulating T cell-dependent cytotoxicity. Notably, FMD and STS are likely to contribute to the killing of cancer cells both by immune-dependent and immune-independent mechanisms, although the effects on 4T1 cells appear to be mostly dependent on the activity of T cells.

HO-1 expression, which is often elevated in tumors, has been shown to be involved in the pathogenesis of several types of cancers (Liu et al., 2004). Here, we show that FMD/STS causes a reduction in HO-1 expression in cancer cells, but not in normal cells. Thus, under FMD conditions, cancer cells but not normal cells are sensitized to chemotherapy, in part by differential regulation of HO-1. In agreement with our results HO-1 downregulation in cancer cells can void their ability to activate Tregs and overcome in situ immunoattack (Otterbein et al., 2000).

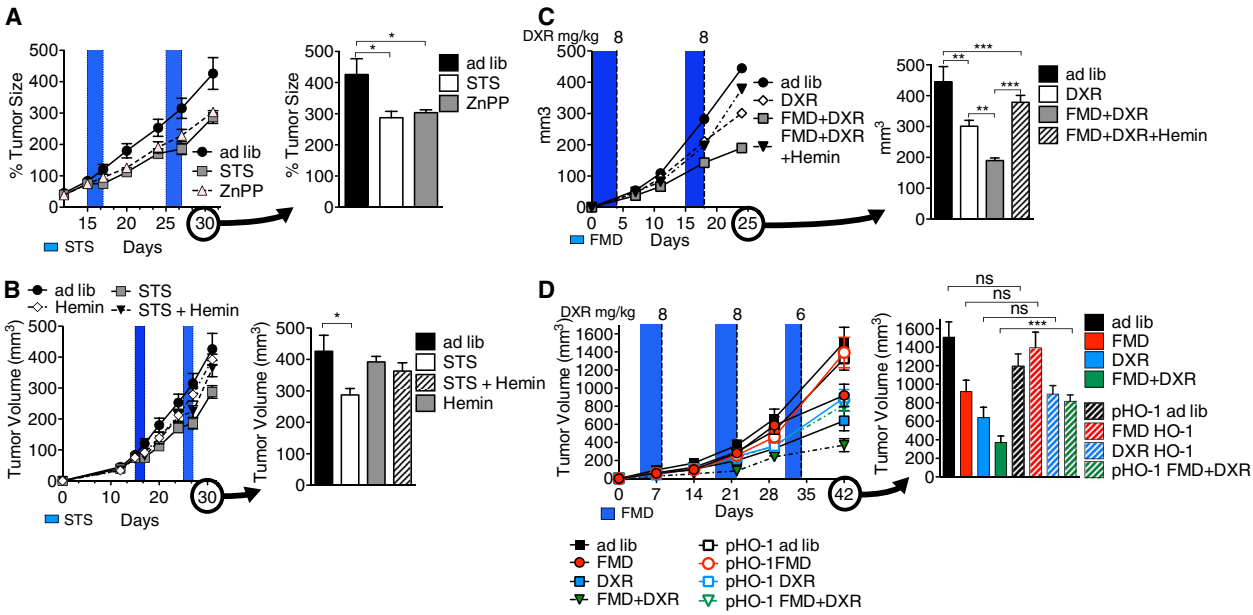

Figure 5. Downregulation of HO-1 in the Tumor during FMD/STS Is Required for the Targeted Attack of Cancer Cells

(A–C) 4T1 tumor-bearing mice were treated with (A) ZnPP (40 mg/kg/day i.p.; n = 7), (B) STS and hemin (30 mg/kg/day i.p.; n = 7), and (C) FMD and hemin and DXR. (D) Mice bearing 4T1 tumors stably overexpressing HO-1 (pHO-1) or empty vector (pEV) were treated with DXR under ad libitum or FMD regimens (n = 10–15) (see Figure 1C).

Data are represented as means ± SEM. One-way ANOVA (Tukey's post-analysis test) was performed. *p < 0.05, **p < 0.01, and ***p < 0.001. See also Figure S6.

Consistent with an involvement of Tregs in HO-1-dependent regulation of DSS, the activation of HO-1 in mice rendered the FMD ineffective in inducing an immune-based attack of cancer cells, while its pharmacological inhibition was sufficient to reduce tumor progression in the absence of an FMD treatment.

Taken together, these results indicate that FMD can enhance the efficacy of chemotherapy by enhancing tumor immunogenicity, in part by an HO-1-dependent mechanism, which promotes the recruitment of cytotoxic $CD8^+$ T cells to the tumor bed and reduces tumor-associated Tregs (Figure 7). Thus, FMD cycles have the potential for clinical application based on the enhancement of T cell-mediated cytotoxicity to cancer cells in the presence or absence of chemotherapy, but may also increase the efficacy of antibodies or other immunological strategies being developed for the treatment of a wide variety of tumors.

EXPERIMENTAL PROCEDURES

Animals

Twelve-week-old BALB/c (wild-type) and BALB/c *nude* mice were purchased from Simonsen Laboratories or from Envigo. Twelve-week-old C57BL/6 female mice were purchased from Charles River Laboratories International. The animals were housed under specific pathogen-free conditions with 12 hr day/light cycles. All the experiments were performed according to procedures approved by USC's Institutional Animal Care and Use Committee.

Diet

Mice were maintained on irradiated TD.7912 rodent chow (Harlan Teklad). In brief, this diet contains 3.75 kcal/g of digestible energy with calories supplied by protein, carbohydrate, and fat in a percent ratio of 25:58:17. Food was provided ad libitum. On average, mice in the control group consumed 14.9 kcal/day (or 3.9 g/day). Our experimental FMD diet is based on a nutritional screen that identified ingredients allowing high nourishment during periods of low calorie consumption (Brandhorst et al., 2013). Before supplying the FMD diet, animals were transferred into fresh cages to avoid feeding on residual chow and coprophagy. The FMD diet consists of two different components designated as day 1 diet and day 2–4 diet that were fed in this order, respectively. The day 1 diet contains 1.88 kcal/g and was designed to adapt the mouse to a period of low caloric intake during the subsequent feeding days. The day 2–4 diet is identical on all feeding days and contains 0.36 kcal/g. The day 1 and day 2–4 diets were fed as the average intake (~4 g) of the control group fed ad libitum every 2 weeks. Due to the different caloric densities of the supplied FMD diet, mice in this cohort had a ~50% reduction in consumed calories on day 1 and consumed 9.7% of the control cohort on days 2–4. Mice consumed all the supplied food on each day of the FMD regimen and showed no signs of food aversion. After the end of the day 2–4 diet, we supplied TD.7912 chow ad libitum for 10 days before starting another FMD cycle.

STS

In the in vivo model, animals underwent complete food deprivation with free access to water for a total of 48–60 hr to allow a 20% bodyweight loss. In order to avoid dehydration, the mice were fed a low caloric hydrogel, which encouraged water consumption. During the STS regimen, mice were individually housed in a clean cage to reduce cannibalism and coprophagy. Body weight was measured immediately before, during, and after fasting. In the in vitro model, FMD-like conditions in cell culture models are referred to as STS (0.5 g/l glucose with 1% fetal bovine serum [FBS]).

Cancer Cell Lines and Tumor Cell Injection

MCF7 human breast adenocarcinoma (gift from Amy Lee, University of Southern California), 4T1-*luc* murine breast cancer (SibTech), and B16 murine melanoma (gift from Noah Craft, UCLA) cell lines were cultured in high glucose (4.5 g/l) DMEM supplemented with 10% FBS (Thermo Fisher Scientific) at 37°C and 5% CO_2. To establish a subcutaneous cancer mouse model, we injected female BALB/c mice or female C57BL/6 mice with 4T1 breast cancer cells or B16 melanoma cells, respectively. Before injection, cells in the log

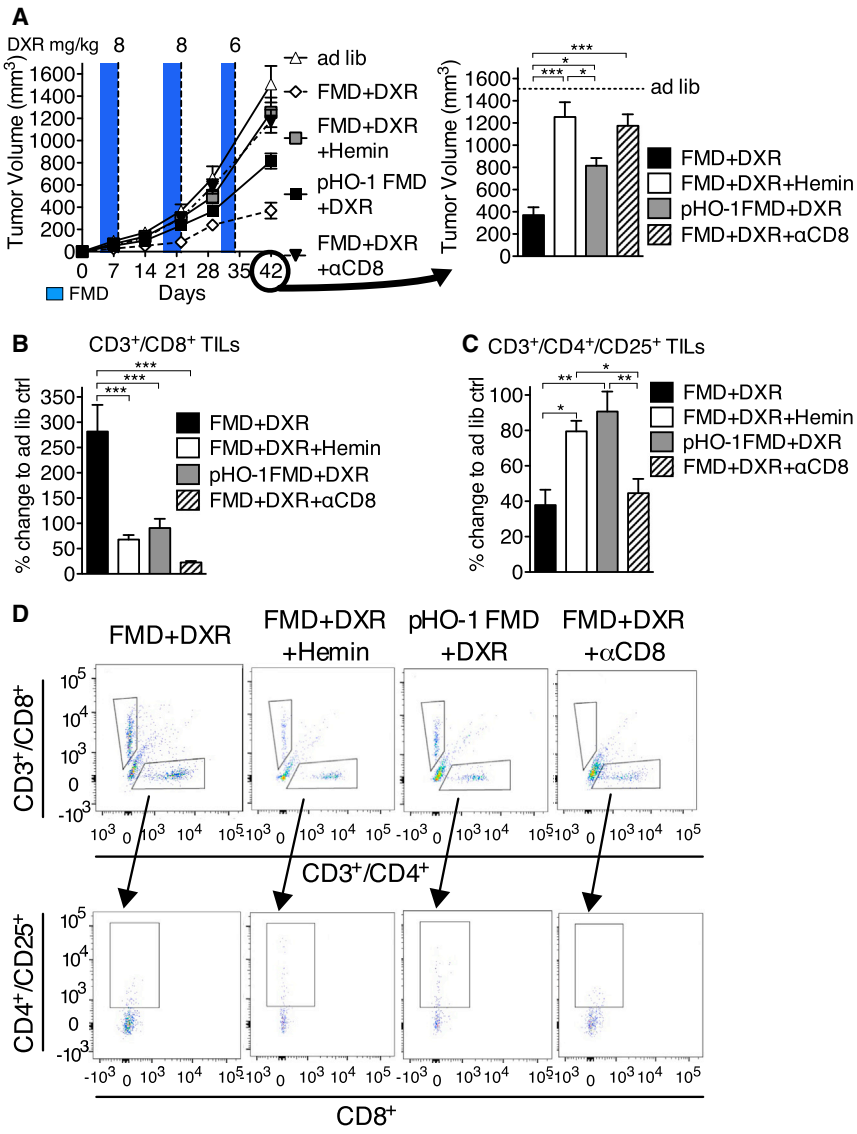

Figure 6. Upregulation or Overexpression of HO-1 Lead to Decreased Infiltration of TILs and Accumulation of Tregs in the Tumor Bed

Mice bearing 4T1 or 4T1-pHO-1 breast tumors under FMD were treated with DXR and either hemin (30 mg/kg/day i.p.) or $CD8^+$ specific neutralizing monoclonal antibodies (αCD8; clone YTS 169.4) (n = 13–15) (see Figures 3F and 5D).

(A) Tumor volumes were measured at multiple time points (left) and immediately before mice were euthanized (right).

(B–D) $CD3^+/CD8^+$ (CTL) and $CD3^+/CD4^+/CD25^+$ (Treg) lymphocytes from the tumor bed were analyzed using FACS.

Data are represented as means ± SEM. One-way ANOVA (Tukey's post-analysis test) was performed. *p < 0.05, ** p < 0.01, and ***p < 0.001.

phase of growth were harvested and suspended in PBS at 2 × 10^6 cells/ml, and 100 μl (2 × 10^5 cells per mouse) were injected subcutaneously in the flank. Body weight was determined periodically, and tumor size was measured with a digital vernier caliper. Tumor volume was calculated with the following equation: tumor volume (mm^3) = (length × width × height)/2, where the height, length, and width are in millimeters.

Immunization with In Vitro Pre-conditioned Cancer Cells

4T1-*luc* murine breast cancer cells (SibTech) were pre-treated in vitro by 48 hr culture under normal conditions (2.0 g/l glucose supplemented with 10% FBS) or "fasting-mimicking conditions" (i.e., STS; 0.5 g/l glucose supplemented with 1% FBS) at 37°C and 5% CO_2. For those cells undergoing DXR pre-conditioning, the drug was added to the medium to a final concentration of 5 μM for the 24 hr preceding the tumor implantation. To induce a "tumor vaccination," the in vitro pre-conditioned cells were injected subcutaneously into the left flank of 12-week-old female BALB/c mice. Specifically, cancer cells pre-conditioned with normal and "fasting-mimicking" medium were inoculated in mice fed ad libitum and belonging to the ad lib and STS groups, respectively. Cells pre-treated in vitro with DXR under the same conditions described above were injected in mice belonging to the DXR and STS + DXR groups. One week after the implantation of pre-treated 4T1 tumor cells, the mice were implanted with untreated 4T1 cells in the right flank. Before injection, cells in the log phase of growth were harvested, analyzed with trypan blue staining, and suspended in PBS at 2 × 10^6 living cells/ml, then 100 μl (2 × 10^5 cells per mouse) were injected subcutaneously in the mouse. It is important to clarify that, for this specific experiment, all mice were fed ad libitum for the whole time and the only difference between one group and the other was the different pre-conditioning of the cancer cells inoculated. All cells were grown to 70% confluency and only live cells, determined by trypan blue exclusion, were used for subcutaneous grafting. An equal number of live cells was injected into each mouse.

Generation of pHO-1 4T1 Cells

4T1-*luc* murine breast cancer (SibTech) cells were transfected with HO-1 plasmid (Suliman et al., 2007), or its parental empty vector, DNA using Lipofectamine 3000. Following incubation at 37°C for 48 hr, the transfected cells were incubated in selection medium containing G418. The selection step was carried on for 7 days and the selecting medium was replaced every 48 hr. Upon seeding, single colonies were grown, selected, and then expanded. The effectiveness of transfection was confirmed with PCR and western blot analyses in some of the clones.

Quantitative PCR

Relative transcript expression levels were measured using RT^2 qPCR Primer Assay for Hmox1 (QIAGEN).

Subcellular Fraction Isolation

For the isolation of cellular fractions, following culture in control and STS medium conditions, 4T1 cells were trypsinized, washed in ice-cold PBS, and processed using a Qproteome Mitochondria Isolation Kit following the manufacturer's recommendations (QIAGEN).

Statistical Analyses

ImageJ software was used for the quantification of the signal and GraphPad Prism v5.0c was used for the graphic representation and statistical analysis of the data. The significance of the differences between groups in mouse experiments was determined using ANOVA analysis in GraphPad Prism v5.0c. Tukey's test was used in the post analysis and the differences were considered significant if the p value was ≤0.05. Comparisons between groups were done with Student's t test using GraphPad Prism v.5.0c. All the

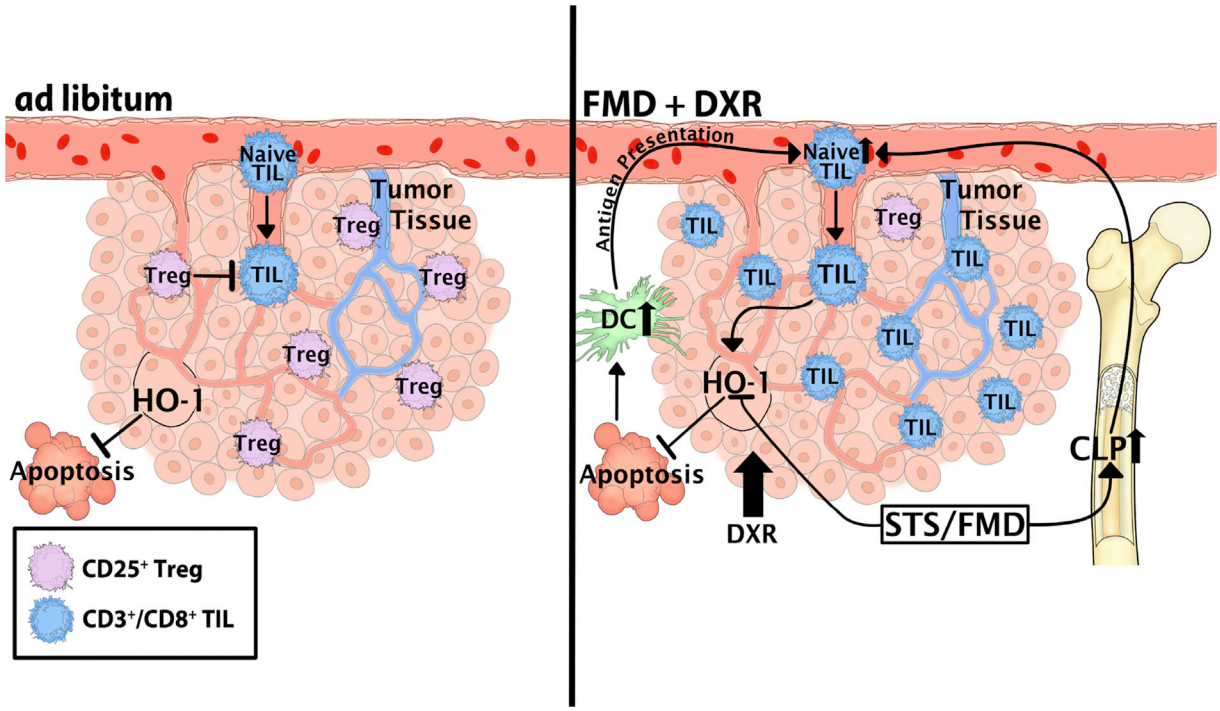

Figure 7. A Model of FMD-Dependent DSS in Tumors

Two scenarios describing the rearrangement of tumor and immune system under different dietary interventions are shown. FMD + DXR increases the immunogenicity of tumors in an HO-1-dependent manner, and increases the recruitment of $CD3^+/CD8^+$ cytotoxic lymphocytes to the tumor bed (TILs), leading to the targeted attack of cancer cells. Such increase of $CD3^+/CD8^+$ TILs is accompanied by the reduction of $CD3^+/CD4^+/CD25^+$ Tregs in the tumor bed. The latter scenario is also associated with an increase of CLP in the bone marrow and of circulating $CD3^+/CD8^+$ cytotoxic lymphocytes. Dendritic cells (DC) can recognize DXR-induced apoptotic tumor cells and stimulate circulating $CD3^+/CD8^+$ CTLs, which, in our model, can be augmented by FMD cycles.

statistical analyses were two-sided and p values ≤ 0.05 were considered significant.

ACCESSION NUMBERS

Microarray data shown in this study have been deposited to Gene Expression Omnibus (GEO), under accession number GEO: GSE28556.

SUPPLEMENTAL INFORMATION

Supplemental Information includes Supplemental Experimental Procedures and six figures and can be found with this article online at http://dx.doi.org/10.1016/j.ccell.2016.06.005.

AUTHOR CONTRIBUTIONS

S.D.B. and C.L. performed most of the experiments and analyses together with C.W.C., A.M.M., R.D.C., R.B., M.C., B.M., and S.B; S.D.B., C.L., and V.D.L. conceived the project; D.B.S., C.L., V.D.L., M.W., and T.M. designed the experiments; S.D.B., C.L., and V.D.L wrote the paper.

ACKNOWLEDGMENTS

This study was funded by NIH grant P01 AG034906 to V.D.L. and subcontract HHSN261201200051C from NCI to M.W. R.d.C and A.M.M. were funded by the Intramural Research Program of the National Institute on Aging, NIH. We thank William Wood, Elin Lehrmann, and Yongqing Zhang for assistance with microarray analyses. V.D.L. and T.M. have equity interest in L-Nutra, a company developing medical food.

Received: June 15, 2015
Revised: January 30, 2016
Accepted: June 10, 2016
Published: July 11, 2016

REFERENCES

Abraham, N.G., and Kappas, A. (2008). Pharmacological and clinical aspects of heme oxygenase. Pharmacol. Rev. *60*, 79–127.

Ahmad, S., Hewett, P.W., Fujisawa, T., Sissaoui, S., Cai, M., Gueron, G., Al-Ani, B., Cudmore, M., Ahmed, S.F., Wong, M.K., et al. (2015). Carbon monoxide inhibits sprouting angiogenesis and vascular endothelial growth factor receptor-2 phosphorylation. Thromb. Haemost. *113*, 329–337.

Alizadeh, D., Trad, M., Hanke, N.T., Larmonier, C.B., Janikashvili, N., Bonnotte, B., Katsanis, E., and Larmonier, N. (2014). Doxorubicin eliminates myeloid-derived suppressor cells and enhances the efficacy of adoptive T-cell transfer in breast cancer. Cancer Res. *74*, 104–118.

Andre, F., Dieci, M.V., Dubsky, P., Sotiriou, C., Curigliano, G., Denkert, C., and Loi, S. (2013). Molecular pathways: involvement of immune pathways in the therapeutic response and outcome in breast cancer. Clin. Cancer Res. *19*, 28–33.

Arinaga, S., Akiyoshi, T., and Tsuji, H. (1986). Augmentation of the generation of cell-mediated cytotoxicity after a single dose of adriamycin in cancer patients. Cancer Res. *46*, 4213–4216.

Balow, J.E., Hurley, D.L., and Fauci, A.S. (1975). Cyclophosphamide suppression of established cell-mediated immunity. Quantitative vs. qualitative changes in lymphocyte populations. J. Clin. Invest. *56*, 65–70.

Bracci, L., Schiavoni, G., Sistigu, A., and Belardelli, F. (2014). Immune-based mechanisms of cytotoxic chemotherapy: implications for the design of novel and rationale-based combined treatments against cancer. Cell Death Differ. *21*, 15–25.

Brandhorst, S., Wei, M., Hwang, S., Morgan, T.E., and Longo, V.D. (2013). Short-term calorie and protein restriction provide partial protection from chemotoxicity but do not delay glioma progression. Exp. Gerontol. *48*, 1120–1128.

Brandhorst, S., Choi, I.Y., Wei, M., Cheng, C.W., Sedrakyan, S., Navarrete, G., Dubeau, L., Yap, L.P., Park, R., Vinciguerra, M., et al. (2015). A periodic diet that mimics fasting promotes multi-system regeneration, enhanced cognitive performance, and healthspan. Cell Metab. *22*, 86–99.

Brusko, T.M., Wasserfall, C.H., Agarwal, A., Kapturczak, M.H., and Atkinson, M.A. (2005). An integral role for heme oxygenase-1 and carbon monoxide in maintaining peripheral tolerance by CD4+CD25+ regulatory T cells. J. Immunol. *174*, 5181–5186.

Burns, W.R., Zhao, Y., Frankel, T.L., Hinrichs, C.S., Zheng, Z., Xu, H., Feldman, S.A., Ferrone, S., Rosenberg, S.A., and Morgan, R.A. (2010). A high molecular weight melanoma-associated antigen-specific chimeric antigen receptor redirects lymphocytes to target human melanomas. Cancer Res. *70*, 3027–3033.

Carmi, Y., Spitzer, M.H., Linde, I.L., Burt, B.M., Prestwood, T.R., Perlman, N., Davidson, M.G., Kenkel, J.A., Segal, E., Pusapati, G.V., et al. (2015). Allogeneic IgG combined with dendritic cell stimuli induce antitumour T-cell immunity. Nature *521*, 99–104.

Casares, N., Pequignot, M.O., Tesniere, A., Ghiringhelli, F., Roux, S., Chaput, N., Schmitt, E., Hamai, A., Hervas-Stubbs, S., Obeid, M., et al. (2005). Caspase-dependent immunogenicity of doxorubicin-induced tumor cell death. J. Exp. Med. *202*, 1691–1701.

Chen, G.G., Liu, Z.M., Vlantis, A.C., Tse, G.M., Leung, B.C., and van Hasselt, C.A. (2004). Heme oxygenase-1 protects against apoptosis induced by tumor necrosis factor-alpha and cycloheximide in papillary thyroid carcinoma cells. J. Cell Biochem. *92*, 1246–1256.

Cheng, C.W., Adams, G.B., Perin, L., Wei, M., Zhou, X., Lam, B.S., Da Sacco, S., Mirisola, M., Quinn, D.I., Dorff, T.B., et al. (2014). Prolonged fasting reduces IGF-1/PKA to promote hematopoietic-stem-cell-based regeneration and reverse immunosuppression. Cell Stem Cell *14*, 810–823.

Choi, B.M., Pae, H.O., Jeong, Y.R., Kim, Y.M., and Chung, H.T. (2005). Critical role of heme oxygenase-1 in Foxp3-mediated immune suppression. Biochem. Biophys. Res. Commun. *327*, 1066–1071.

El Andaloussi, A., and Lesniak, M.S. (2007). CD4+ CD25+ FoxP3+ T-cell infiltration and heme oxygenase-1 expression correlate with tumor grade in human gliomas. J. Neurooncol. *83*, 145–152.

Hirai, K., Sasahira, T., Ohmori, H., Fujii, K., and Kuniyasu, H. (2007). Inhibition of heme oxygenase-1 by zinc protoporphyrin IX reduces tumor growth of LL/2 lung cancer in C57BL mice. Int. J. Cancer *120*, 500–505.

Hsu, F.F., Yeh, C.T., Sun, Y.J., Chiang, M.T., Lan, W.M., Li, F.A., Lee, W.H., and Chau, L.Y. (2015). Signal peptide peptidase-mediated nuclear localization of heme oxygenase-1 promotes cancer cell proliferation and invasion independent of its enzymatic activity. Oncogene *34*, 2360–2370.

Inoue, S., Setoyama, Y., and Odaka, A. (2014). Doxorubicin treatment induces tumor cell death followed by immunomodulation in a murine neuroblastoma model. Exp. Ther. Med. *7*, 703–708.

Issa-Nummer, Y., Darb-Esfahani, S., Loibl, S., Kunz, G., Nekljudova, V., Schrader, I., Sinn, B.V., Ulmer, H.U., Kronenwett, R., Just, M., et al. (2013). Prospective validation of immunological infiltrate for prediction of response to neoadjuvant chemotherapy in HER2-negative breast cancer–a substudy of the neoadjuvant GeparQuinto trial. PLoS One *8*, e79775.

Lee, C., Safdie, F.M., Raffaghello, L., Wei, M., Madia, F., Parrella, E., Hwang, D., Cohen, P., Bianchi, G., and Longo, V.D. (2010). Reduced levels of IGF-I mediate differential protection of normal and cancer cells in response to fasting and improve chemotherapeutic index. Cancer Res. *70*, 1564–1572.

Lee, C., Raffaghello, L., Brandhorst, S., Safdie, F.M., Bianchi, G., Martin-Montalvo, A., Pistoia, V., Wei, M., Hwang, S., Merlino, A., et al. (2012). Fasting cycles retard growth of tumors and sensitize a range of cancer cell types to chemotherapy. Sci. Transl. Med. *4*, 124ra127.

Liu, Z.M., Chen, G.G., Ng, E.K., Leung, W.K., Sung, J.J., and Chung, S.C. (2004). Upregulation of heme oxygenase-1 and p21 confers resistance to apoptosis in human gastric cancer cells. Oncogene *23*, 503–513.

Liu, Y., Liang, Y., Zheng, T., Yang, G., Zhang, X., Sun, Z., Shi, C., and Zhao, S. (2011). Inhibition of heme oxygenase-1 enhances anti-cancer effects of arsenic trioxide on glioma cells. J. Neurooncol. *104*, 449–458.

Maines, M.D. (1988). Heme oxygenase: function, multiplicity, regulatory mechanisms, and clinical applications. FASEB J. *2*, 2557–2568.

Maude, S.L., Frey, N., Shaw, P.A., Aplenc, R., Barrett, D.M., Bunin, N.J., Chew, A., Gonzalez, V.E., Zheng, Z., Lacey, S.F., et al. (2014). Chimeric antigen receptor T cells for sustained remissions in leukemia. N. Engl. J. Med. *371*, 1507–1517.

Metz, R., Duhadaway, J.B., Rust, S., Munn, D.H., Muller, A.J., Mautino, M., and Prendergast, G.C. (2010). Zinc protoporphyrin IX stimulates tumor immunity by disrupting the immunosuppressive enzyme indoleamine 2,3-dioxygenase. Mol. Cancer Ther. *9*, 1864–1871.

Michaud, M., Martins, I., Sukkurwala, A.Q., Adjemian, S., Ma, Y., Pellegatti, P., Shen, S., Kepp, O., Scoazec, M., Mignot, G., et al. (2011). Autophagy-dependent anticancer immune responses induced by chemotherapeutic agents in mice. Science *334*, 1573–1577.

Orsini, F., Pavelic, Z., and Mihich, E. (1977). Increased primary cell-mediated immunity in culture subsequent to adriamycin or daunorubicin treatment of spleen donor mice. Cancer Res. *37*, 1719–1726.

Otterbein, L.E., Bach, F.H., Alam, J., Soares, M., Tao Lu, H., Wysk, M., Davis, R.J., Flavell, R.A., and Choi, A.M. (2000). Carbon monoxide has anti-inflammatory effects involving the mitogen-activated protein kinase pathway. Nat. Med. *6*, 422–428.

Pardoll, D.M. (2012). Immunology beats cancer: a blueprint for successful translation. Nat. Immunol. *13*, 1129–1132.

Raffaghello, L., Lee, C., Safdie, F.M., Wei, M., Madia, F., Bianchi, G., and Longo, V.D. (2008). Starvation-dependent differential stress resistance protects normal but not cancer cells against high-dose chemotherapy. Proc. Natl. Acad. Sci. USA *105*, 8215–8220.

Rasmussen, L., and Arvin, A. (1982). Chemotherapy-induced immunosuppression. Environ. Health Perspect. *43*, 21–25.

Rock, K.L., and Shen, L. (2005). Cross-presentation: underlying mechanisms and role in immune surveillance. Immunol. Rev. *207*, 166–183.

Safdie, F.M., Dorff, T., Quinn, D., Fontana, L., Wei, M., Lee, C., Cohen, P., and Longo, V.D. (2009). Fasting and cancer treatment in humans: a case series report. Aging *1*, 988–1007.

Suliman, H.B., Carraway, M.S., Ali, A.S., Reynolds, C.M., Welty-Wolf, K.E., and Piantadosi, C.A. (2007). The CO/HO system reverses inhibition of mitochondrial biogenesis and prevents murine doxorubicin cardiomyopathy. J. Clin. Invest. *117*, 3730–3741.

Tertil, M., Golda, S., Skrzypek, K., Florczyk, U., Weglarczyk, K., Kotlinowski, J., Maleszewska, M., Czauderna, S., Pichon, C., Kieda, C., et al. (2015). Nrf2-heme oxygenase-1 axis in mucoepidermoid carcinoma of the lung: antitumoral effects associated with down-regulation of matrix metalloproteinases. Free Radic. Biol. Med. *89*, 147–157.

Vesely, M.D., Kershaw, M.H., Schreiber, R.D., and Smyth, M.J. (2011). Natural innate and adaptive immunity to cancer. Annu. Rev. Immunol. *29*, 235–271.

Wegiel, B., Gallo, D., Csizmadia, E., Harris, C., Belcher, J., Vercellotti, G.M., Penacho, N., Seth, P., Sukhatme, V., Ahmed, A., et al. (2013). Carbon monoxide expedites metabolic exhaustion to inhibit tumor growth. Cancer Res. *73*, 7009–7021.

Weinblatt, M.E., Coblyn, J.S., Fox, D.A., Fraser, P.A., Holdsworth, D.E., Glass, D.N., and Trentham, D.E. (1985). Efficacy of low-dose methotrexate in rheumatoid arthritis. N. Engl. J. Med. *312*, 818–822.

Weiner, H.L., and Cohen, J.A. (2002). Treatment of multiple sclerosis with cyclophosphamide: critical review of clinical and immunologic effects. Mult. Scler. *8*, 142–154.

Wolchok, J.D., Kluger, H., Callahan, M.K., Postow, M.A., Rizvi, N.A., Lesokhin, A.M., Segal, N.H., Ariyan, C.E., Gordon, R.A., Reed, K., et al. (2013). Nivolumab plus ipilimumab in advanced melanoma. N. Engl. J. Med. *369*, 122–133.

Xia, Z.W., Zhong, W.W., Meyrowitz, J.S., and Zhang, Z.L. (2008). The role of heme oxygenase-1 in T cell-mediated immunity: the all encompassing enzyme. Curr. Pharm. Des. *14*, 454–464.

Zitvogel, L., Tesniere, A., and Kroemer, G. (2006). Cancer despite immunosurveillance: immunoselection and immunosubversion. Nat. Rev. Immunol. *6*, 715–727.

Zitvogel, L., Apetoh, L., Ghiringhelli, F., and Kroemer, G. (2008). Immunological aspects of cancer chemotherapy. Nat. Rev. Immunol. *8*, 59–73.

Cancer Cell, Volume *30*

Supplemental Information

Fasting-Mimicking Diet Reduces HO-1 to Promote T Cell-Mediated Tumor Cytotoxicity

Stefano Di Biase, Changhan Lee, Sebastian Brandhorst, Brianna Manes, Roberta Buono, Chia-Wei Cheng, Mafalda Cacciottolo, Alejandro Martin-Montalvo, Rafael de Cabo, Min Wei, Todd E. Morgan, and Valter D. Longo

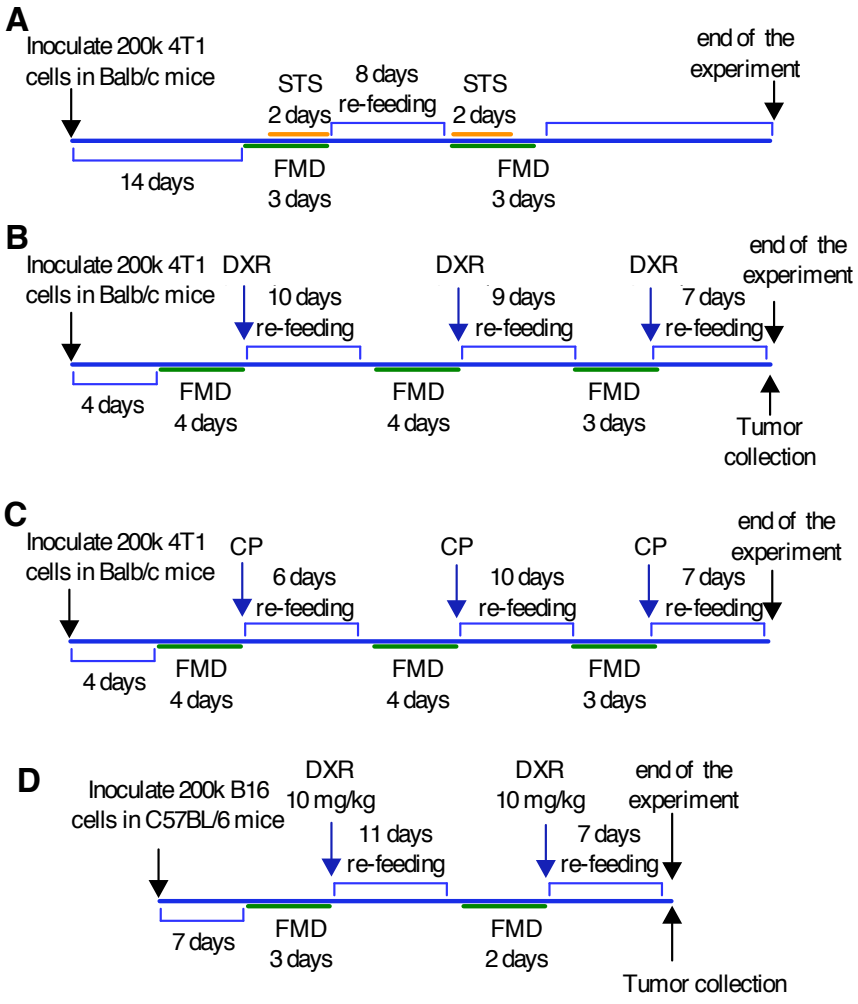

Figure S1. Related to Figure 1 . Schematic representation of tumor progression experiments. Schematics of the experimental schedules in Figure 1 A, C-E are shown in A, B, C, and D, respectively**.** (**A**, **B**, and **C**) 12-week old female BALB/c and (**D**) C57BL/6 mice were inoculated with (**A**, **B**, and **C**) 200,000 4T1 murine breast cancer or (**D**) B16 murine melanoma cells in the right flank. FMD and STS groups underwent 3-4 days (FMD) or 2 days (STS) of dietary intervention followed (right at the end of the regimen) by DXR or CP injection. Between FMD/STS cycles, the animals were ad lib fed for a period of 8-11 days to allow for the recovery of the body weight lost. The third cycle of FMD was reduced to 3 days because of the faster rate of body weight loss. 7 days following the last administration of chemotherapy the animals were euthanized.

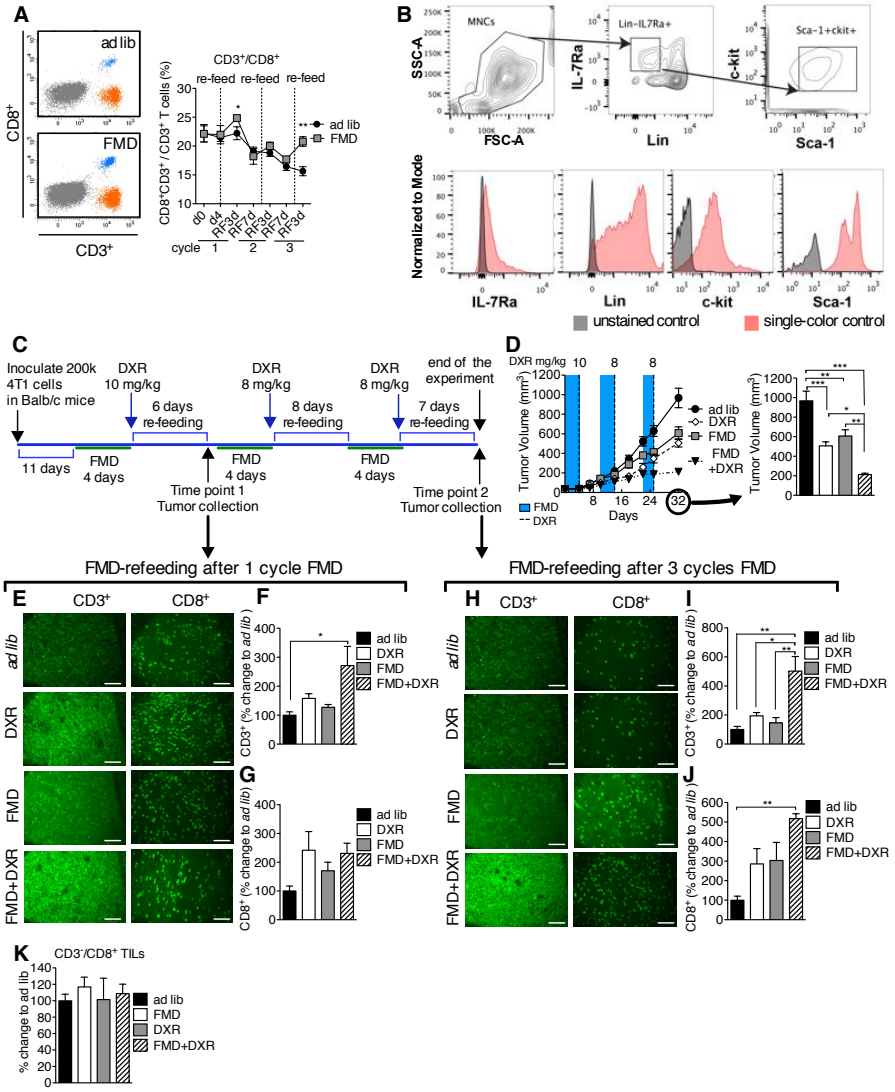

Figure S2. Related to Figure 2. The effect of FMD on CD3$^+$/CD8$^+$ TILs .
(A) Blood from BALB/c mice undergoing *ad lib* and FMD regimens was collected at different time points and analyzed with FACS (n=6) to assess levels of CD3$^+$/CD8$^+$ circulating cells. (**B**) Gating strategy for FACS analysis used to quantify Common Lymphoid Progenitors (CLP) from bone marrow collected from BALB/c mice undergoing FMD/DXR treatments (described in Figure S3A (n=6). **(C)** 7-month old female BALB/c mice were inoculated with 200,000 4T1 murine breast cancer cells in the right flank (n=10). One week following the inoculation, the animals were divided in the following groups: *ad lib* (*ad libitum* feeding), FMD, DXR and FMD+DXR. At this point the FMD groups underwent 4 days of dietary intervention followed by DXR injection at the end of FMD (day 4). Between FMD cycles, the animals were *ad lib* fed for a period of 8 to 11 days to allow for the recovery of the body weight lost. (**D**) Tumor progression and tumor volume at the end of the experiment. Tumor tissue was collected 7 days following the first DXR injection (time point 1) and 7 days following the third DXR injection (time point 2), processed and analyzed to assess the levels of tumor infiltrating lymphocytes (TILs). Infiltration of CD3$^+$ and CD8$^+$ TILs are shown at (**E-G**) time point 1 and (**H-J**) time point 2 (Scale bars, 75 µm). (**K**) FACS analysis of tumor-infiltrating CD3$^-$/CD8$^+$ lymphocites collected from animals in figure 6A is shown. Data represented as mean ± SEM. One-way ANOVA (Tukey post-analysis test) was performed. p-values <0.05, 0.01 and 0.001 are indicated as *, **, and ***, respectively.

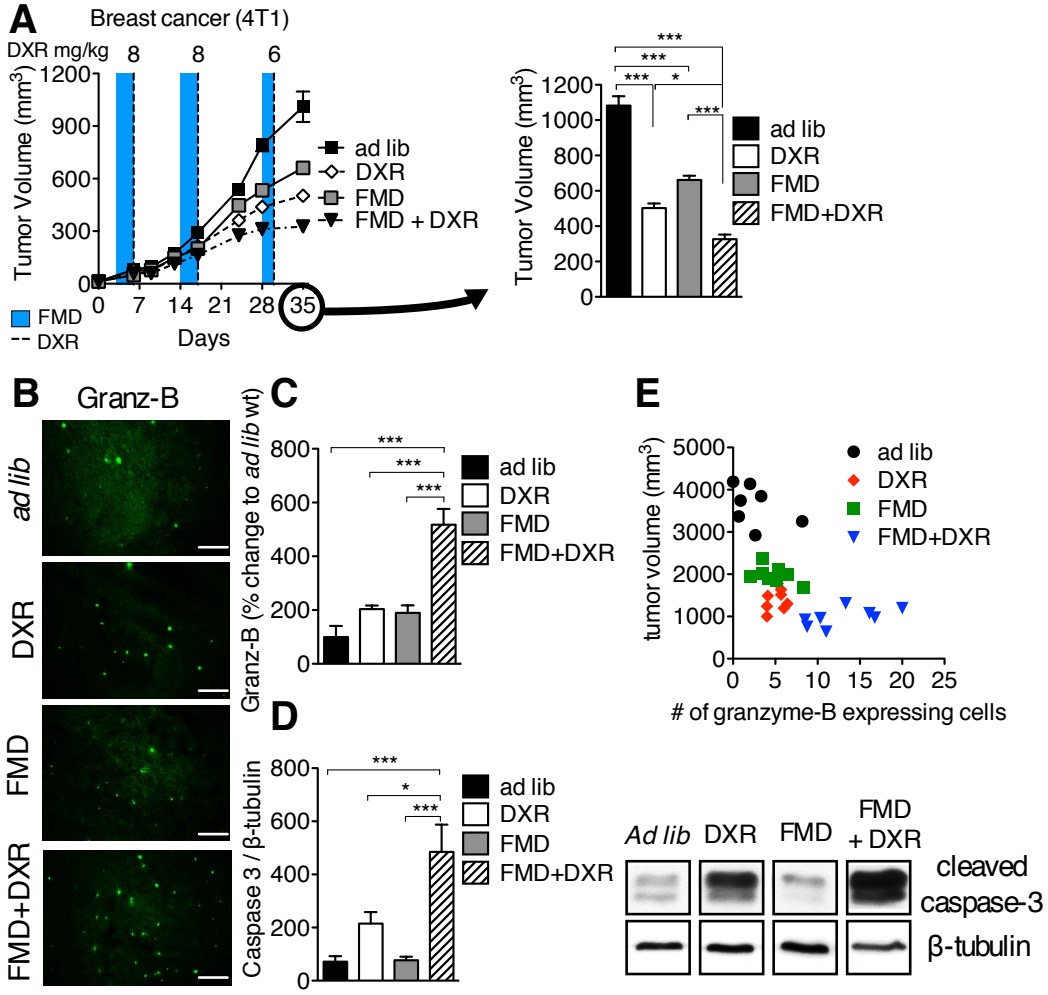

Figure S3. Related to Figure 3. Cytotoxicity markers are activated in TIL infiltrated 4T1 tumors.

12-week old female BALB/c mice were grafted with 200,00 4T1 murine breast cancer cells and underwent FMD/re-feeding regimen and were administrated DXR i.v. at the end of each cycle (n=15). (**A**) Tumor progression and tumor volumes measured at the end of the experiment. Tumors were collected at the end of the experiment and analyzed by (**B-C**) IHC to assess granzyme-B levels (Scale bars, 75 µm), and by (**D**) Western blotting to determine cleaved caspase-3 levels (n=8) (Blot was captured on film, and unedited, representative bands are shown). (**E**) Association between tumor volume at the end of the experiment and granzyme-B levels. Data represented as mean ± SEM. One-way ANOVA (Tukey post-analysis test) was performed. p-values <0.05, 0.01 and 0.001 are indicated as *, **, and ***, respectively.

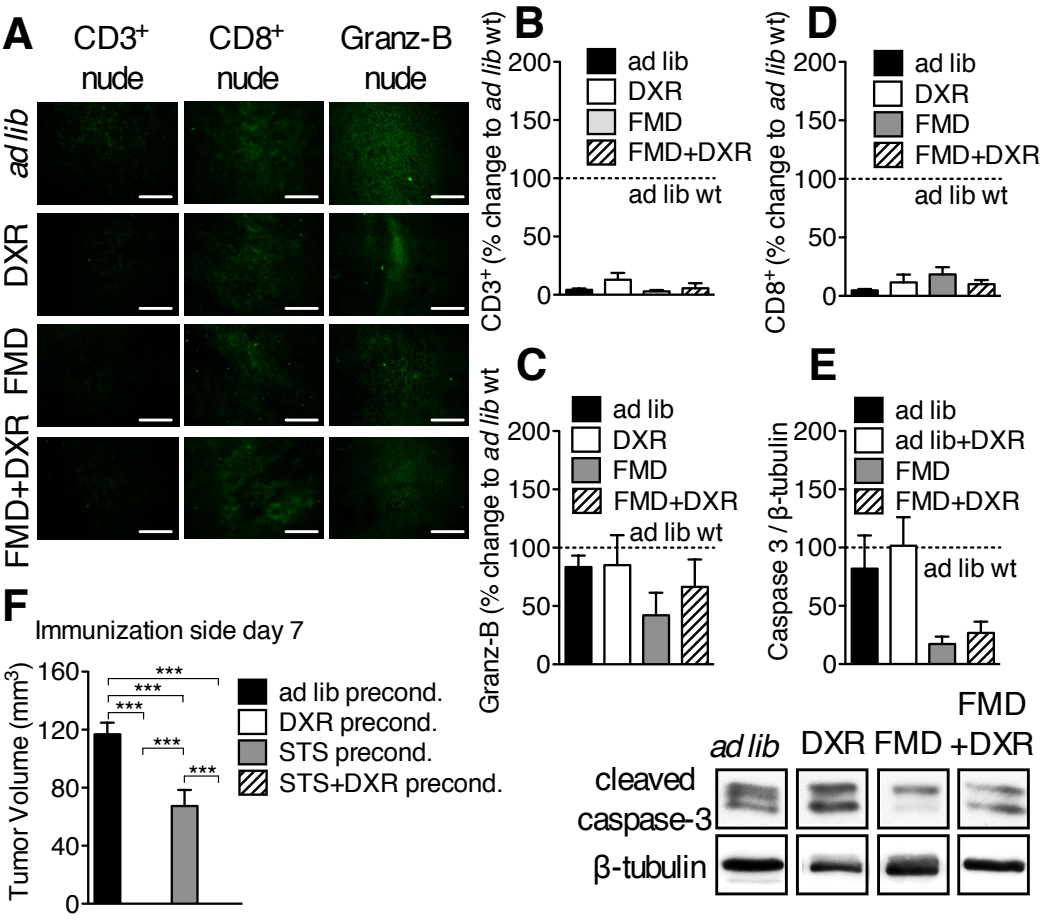

Figure S4. Consecutive cycles of FMD+DXR alter intratumoral lymphocyte composition. Tumor tissues collected at the end of the experiment shown in Figure 2B were analyzed by (**A-D**) IHC to assess $CD3^+$ and $CD8^+$ TILs, and granzyme B (Scale bars, 75 μm), and by (**E**) Western blotting to assess caspase-3 levels (n=8) (Blot was captured on film, and unedited, representative bands are shown). (**F**) 4T1 cells pre-conditioned *in vitro* were inoculated in the left flank of BALB/c mice for the immunization experiment described in Figure 3I. Tumor volume at 7 days after inoculation is shown. Data represented as mean ± SEM. One-way ANOVA (Tukey post-analysis test) was performed. p-values <0.05, 0.01 and 0.001 are indicated as *, **, and ***, respectively.

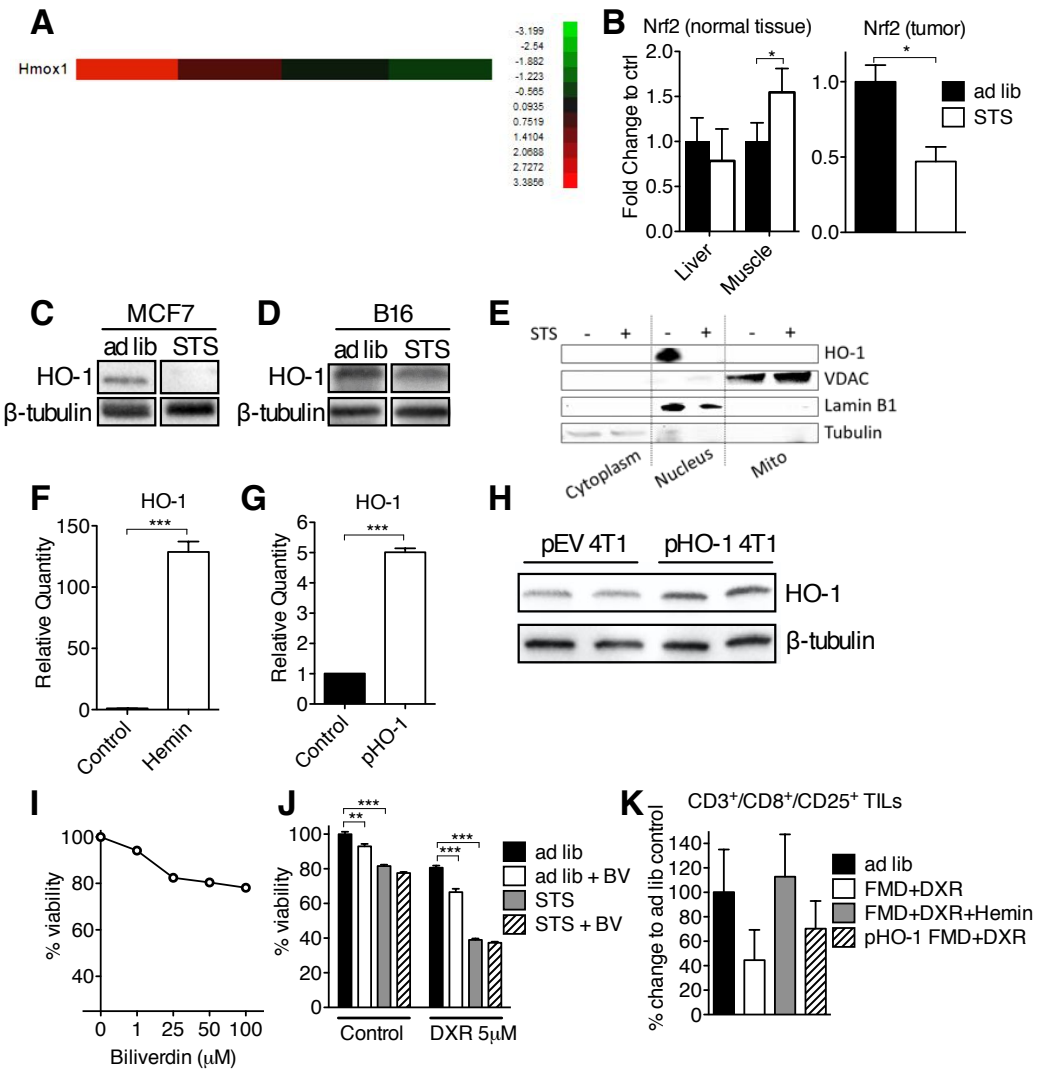

Figure S5. Related to Figure 4. Fasting differentially reduces tumor HO-1 and Nrf2 expression levels *in vivo* and *in vitro*.

Grafted breast tumor (4T1) and normal (liver and skeletal muscle) tissues were collected following a 48-hour STS and subject to an unbiased global gene expression microarray (n=6). (**A**) A representative image of Hmox1 (HO-1) levels from the microarray. (**B**) NRF2 expression levels were analyzed by qRT-PCR (n=3). (**C, D**) Down-regulation of HO-1 during *in vitro* STS is also shown by Western blotting in human breast adenocarcinoma (MCF7) and murine melanoma (B16) cells (n=3) (Blot was captured with Bio-Rad ChemiDoc, and unedited, representative bands are shown). (**E**) Subcellular localization of HO-1 protein in 4T1 cell before and after a 24-hour *in vitro* STS; voltage-dependent anion channel (VDAC; mitochondrial marker), lamin B1 (nuclear marker), and tubulin (cytoplasmic marker). (**F**) Hemin (20 uM) increased HO-1 expression levels in 4T1 cells as determined by qRT-PCR (n=3). (**G, H**) 4T1 cells that were stably transfected to over-express HO-1 had increased HO-1 expression as determined by (**G**) qRT-PCR and (**H**) Western blotting (n=3). (**I**) *In vitro* dose response to increasing concentrations of biliverdin ranging from 0-100 μM. **(J)** *In vitro* viability in response to biliverdin (BV) 1μM in 4T1 cells with and without STS and/or DXR, determined by MTT reduction (n=3). **(K)** FACS analysis of tumor-infiltrating $CD3^+/CD8^+/CD25^+$ Treg lymphocites collected from animals in figure 6A is shown. Data represented as mean ± SEM. Student's t-test was performed to compare two groups. p-values <0.05, 0.01 and 0.001 are indicated as *, **, and ***, respectively.

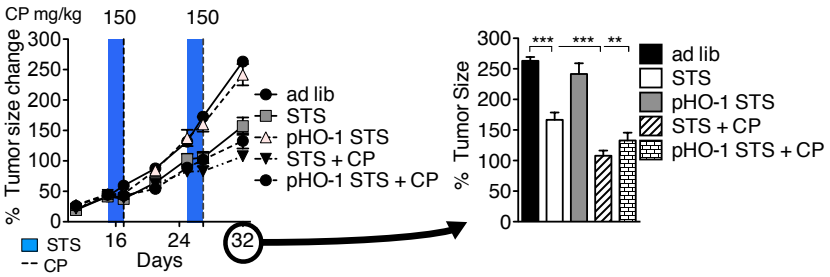

Figure S6. Related to Figure 5. STS sensitizes grafted 4T1 tumors to CP in a HO-1-dependent manner.

12-week old female BALB/c mice were grafted with 200,000 4T1 murine breast cancer cells that were stable transfected with a HO-1 expression (pHO-1) (n=10). Mice underwent two cycles of STS (48-hours) with or without CP (150 mg/kg, IP). Tumor progression was measured at multiple time points (left panel), including immediately prior to euthanasia (right panel). Data represented as mean ± SEM. Student's t-test was performed to compare two groups. p-values <0.05, 0.01 and 0.001 are indicated as *, **, and ***, respectively.

SUPPLEMENTAL EXPERIMENTAL PROCEDURES

Doxorubicin administration: Doxorubicin HCL (DXR) (Pfizer Inc.) 2 mg/ml was injected intravenously (IV) at concentrations that varied based on the experiment setup and between animal strains (see results section for doses).

Cyclophosphamide administration: Upon reconstitution in sterile saline, cyclophosphamide (CP) (Baxter Healthcare Corp.) was injected intraperitoneally (IP) at concentration of 150 mg/kg per mouse.

Hemin administration: Hemin (Sigma-Aldrich Co.) was dissolved in 0.7N NH_4OH to final concentration of 50 mg/ml (stock solution). Working solution was prepared daily by diluting stock solution 1:10 in sterile saline. Hemin was administrated IP twice a day at 15 mg/kg (total of 30 mg/kg daily). Control mice were daily-injected IP with vehicle.

Zinc protoporphyrin administration: Zinc protoporphyrin (ZnPP) (Sigma-Aldrich Co.) was dissolved in DMSO to final concentration of 50 mg/ml (stock solution). Working solution was prepared daily by diluting stock solution in sterile saline. ZnPP was administrated IP once a day. Control mice were daily-injected IP with vehicle.

Biliverdin in vitro treatment: Biliverdin hydrochloride (Sigma-Aldrich Co.) was dissolved in DMSO to final concentration of 50 mg/ml (stock solution). For the *in vitro* use, the stock solution was dissolved in culturing media to a final concentration of 1-100μM.

Immunohistochemical Analysis: Tumor tissues were collected and snap frozen immediately after animal sacrifice and stored at -80°C until processed on a Leica CM1800 cryostat where 20 μm sections were serially collected on glass slides. The slides were fixed in 4% paraformaldehyde for 15 minutes, permeabilized in 1% Nonidet P-40 (Sigma-Aldrich) and finally blocked in 5% normal goat serum.

The slides were then incubated overnight at 4°C with either one of the following antibodies: CD3, CD8 (Abcam plc), or granzyme-B (Cell Signaling Technology) primary antibodies. The incubation with secondary antibody was performed 1 hour at RT with either goat anti-mouse (Alexa Fluor® 488) or goat anti-rabbit (Alexa Fluor® 594). Glass slides from B16 tumors were prepared with mounting media containing DAPI (Abcam plc). Infiltration of positive cells in the tissue was detected with fluorescence microscopy (Nikon TE-DH) and then quantified with ImageJ (NIH software).

Protein Extraction and Western Blot Analysis: Tumor tissue was collected immediately after mouse sacrifice at the specified time points. The tissue was snap frozen in liquid nitrogen and stored at -80°C until utilized for the analysis. For the total protein extraction, the tumor tissue was homogenized in presence of RIPA buffer (EMD Millipore), protease- and phosphatase inhibitors (Sigma Aldrich). Total protein extracts were quantified with BCA assay (Thermo Scientific Pierce), dissolved in NuPAGE buffer (life technologies) and denatured at 100°C. 40µg of total proteins were resolved in 18% polyacrylamide gel in presence of SDS and transferred to PVDF membrane before blocking with 5% milk in T-PBS. The membrane was incubated overnight at 4°C with either one of the following primary antibodies: Caspase-3, HO-1, Lamin B1, VDAC and β-tubulin (Cell Signaling Technologies). The incubation with secondary antibody anti-rat or anti-goat (Jackson ImmunoResearch Laboratories, Inc.) was performed for 1h at RT. The membrane was incubated with peroxidase substrate for enhanced chemiluminescence (ECL) for 2 minutes at room temperature and detection was performed by exposing the membrane to film (Figure S3D and S4E) or by detection with Bio-Rad ChemiDoc (Figure 4B, S5C, D, and H). Canon LiDE25 scanner was used for the acquisition of the films and all the raw images were inverted and quantified with ImageJ (NIH software). Raw images from Bio-Rad ChemiDoc were unedited and analyzed directly with ImageJ for quantification. For presentation purpose, representative images of bands belonging to each experimental group were collected and placed together in the figure. The high

number of samples analyzed has required the use of multiple blots, which were processed in parallel following identical conditions. Because of the arrangement of the running lanes on the western blot, bands depicted to be next to each other in the final image might have been on different positions on the blot, or from different blots.

$CD8^+$ cells in vivo depletion: Complete depletion of $CD8^+$ CTL was achieved by intraperitoneal administration of neutralizing monoclonal antibody (αCD8; clone YTS 169.4) or rat IgG (BioXCell, USA) every 4 days. The depletion of circulating $CD8^+$ CTL over time was confirmed by FACS analysis. Lymphocytes from mice were collected using Histopaque 1077 following manufacturer's protocol (Sigma Aldrich, USA).

Flow cytometric analysis for CLP and T cells: Bone marrow cells collected from femurs and tibia were stained with antibodies against lineage markers (APC-Cy7), Sca-1(AF-700), C-kit(APC) and IL-7Ra(PE-Cy7). Peripheral blood cells collected from the tail vein were stained with antibodies against CD8a(AF488) and CD3(APC), according to manufacturer's instructions. All cell acquisition was performed with BD LSR II flow cytometer and analyzed with FACSDiva software (BD Biosciences, San Jose, CA). For the analysis of TILs, upon surgical removal the tumor was washed in ice-cold PBS, was mechanically minced to small fragments and incubated for 1h at 37°C under agitation with collagenase IV (Worthington; 300 units/mL in serum free DMEM) for enzymatic digestion. The digested tissue was then filtered and the isolated cells were washed and incubated with anti CD8, CD3, CD4 and CD25 antibodies (eBioscience, Inc.).

Microarray analysis: RNA from tissues was isolated according the procedures described by the manufacturer using the RNeasy kit (Qiagen). Then, RNA was hybridized to BD-202-0202 chips from Illumina Beadchips. Raw data were

subjected to Z normalization as described (Cheadle et al., 2003). Briefly, for each pathway under each pair of conditions, a Z score was computed as [Z (pathway) = (sm mu)*pow(m,0.5)/delta], where mu = mean Z score of all gene symbols on the microarray, delta = standard deviation of Z scores of all gene symbols on the microarray, sm = mean Z score of gene symbols comprising one pathway present on the microarray, and m = number of gene symbols in a pathway present on the microarray. For each Z (pathway) a p value was also computed in JMP 6.0 to test for the significance of the Z score obtained. These tools are part of DIANE 1.0 and are available at http://www.grc.nia.nih.gov/branches/rrb/dna/diane_software.pdf. Parameterized significant analysis is finished according to the SAM protocol (Tusher et al., 2001) with ANOVA filtering (ANOVA $p<0.05$). Significant genes are selected for each pairwise comparison. Gene set enrichment was tested using the PAGE method as previously described (Kim and Volsky, 2005). Figures were selected based on the names and descriptions provided by Gene Ontology Database and Pathway Data Set (Subramanian et al., 2005). Further gene regularly relation and canonic pathway analysis is done by the Ingenuity Pathway Analysis System (Ingenuity Systems). All raw data are available in the GEO database.

SUPPLEMENTAL REFERENCES

Cheadle, C., Vawter, M. P., Freed, W. J., and Becker, K. G. (2003). Analysis of microarray data using Z score transformation. The Journal of molecular diagnostics : JMD *5*, 73-81.

Kim, S. Y., and Volsky, D. J. (2005). PAGE: parametric analysis of gene set enrichment. BMC bioinformatics *6*, 144.

Subramanian, A., Tamayo, P., Mootha, V. K., Mukherjee, S., Ebert, B. L., Gillette, M. A., Paulovich, A., Pomeroy, S. L., Golub, T. R., Lander, E. S., and Mesirov, J. P. (2005). Gene set enrichment analysis: a knowledge-based approach for interpreting genome-wide expression profiles. Proc Natl Acad Sci U S A *102*, 15545-15550.

Tusher, V. G., Tibshirani, R., and Chu, G. (2001). Significance analysis of microarrays applied to the ionizing radiation response. Proc Natl Acad Sci U S A *98*, 5116-5121.